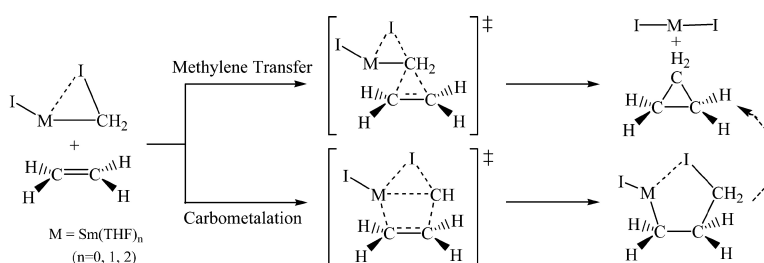


## Theoretical Study of Samarium (II) Carbenoid (ISmCHI) Promoted Cyclopropanation Reactions with Ethylene and the Effect of THF Solvent on the Reaction Pathways

Cunyuan Zhao, Dongqi Wang, and David Lee Phillips

*J. Am. Chem. Soc.*, **2003**, 125 (49), 15200-15209 • DOI: 10.1021/ja030280t • Publication Date (Web): 12 November 2003

Downloaded from <http://pubs.acs.org> on March 30, 2009



### More About This Article

Additional resources and features associated with this article are available within the HTML version:

- Supporting Information
- Access to high resolution figures
- Links to articles and content related to this article
- Copyright permission to reproduce figures and/or text from this article

[View the Full Text HTML](#)



## Theoretical Study of Samarium (II) Carbenoid (ISmCH<sub>2</sub>I) Promoted Cyclopropanation Reactions with Ethylene and the Effect of THF Solvent on the Reaction Pathways

Cunyuan Zhao,<sup>†,‡</sup> Dongqi Wang,<sup>†</sup> and David Lee Phillips\*<sup>†,‡</sup>

Contribution from the Department of Chemistry, University of Hong Kong, Pokfulam Road, Hong Kong, P. R. China, and Department of Chemistry, Northwest Normal University, Lanzhou, 730070, P. R. China.

Received May 6, 2003; E-mail: phillips@hku.hk

**Abstract:** A computational study of the cyclopropanation reactions of divalent samarium carbenoid ISmCH<sub>2</sub>I with ethylene is presented. The reaction proceeds through two competing pathways: methylene transfer and carbometalation. The ISmCH<sub>2</sub>I species was found to have a "samarium carbene complex" character with properties similar to previously investigated lithium carbenoids (LiCH<sub>2</sub>X where X = Cl, Br, I). The ISmCH<sub>2</sub>I carbenoid was found to be noticeably different in structure with more electrophilic character and higher chemical reactivity than the closely related classical Simmons–Smith (IZnCH<sub>2</sub>I) carbenoid. The effect of THF solvent was investigated by explicit coordination of the solvent THF molecules to the Sm (II) center in the carbenoid. The ISmCH<sub>2</sub>I/(THF)<sub>n</sub> (where n = 0, 1, 2) carbenoid methylene transfer pathway barriers to reaction become systematically lower as more THF solvent is added (from 12.9 to 14.5 kcal/mol for no THF molecules to 8.8 to 10.7 kcal/mol for two THF molecules). In contrast, the reaction barriers for cyclopropanation via the carbometalation pathway remain high (> 15 kcal/mol). The computational results are briefly compared to other carbenoid reactions and related species.

### Introduction

Cyclopropane moieties have been found in a wide range of natural and unnatural compounds that exhibit important biological activities and in an array of substances used as starting materials and intermediates in organic synthesis.<sup>1–30</sup> This has mo-

tivated a large number of research groups to develop new and wide-ranging methods to produce cyclopropanated products.<sup>1–61</sup>

- <sup>†</sup> Department of Chemistry, University of Hong Kong.  
<sup>‡</sup> Department of Chemistry, Northwest Normal University.
- (1) *The Chemistry of the Cyclopropyl Group*; Rappoport, Z., Ed.; Wiley: Chichester, 1987.
  - (2) Fritsch, H.; Leutenegger, U.; Pfaltz, A. *Angew. Chem., Int. Ed. Engl.* **1986**, *25*, 1005–1006.
  - (3) Fritsch, H.; Leutenegger, U.; Pfaltz, A. *Helv. Chim. Acta* **1988**, *71*, 1553–1565.
  - (4) Lowenthal, R. E.; Abiko, A.; Masamune, S. *Tetrahedron Lett.* **1990**, *31*, 6005–6008.
  - (5) Evans, D. A.; Woerpel, K. A.; Hinman, M. M.; Faul, M. M. *J. Am. Chem. Soc.* **1991**, *113*, 726–728.
  - (6) Müller, D.; Umbrecht, G.; Weber, B.; Pfaltz, A. *Helv. Chim. Acta* **1991**, *74*, 232–240.
  - (7) Rodriguez, J. B.; Marquez, V. E.; Nicklaus, M. C.; Barchi, J. J., Jr.; *Tetrahedron Lett.* **1993**, *34*, 6233–6236.
  - (8) Zhao, Y.; Yang, T.-F.; Lee, M.; Chun, B. K.; Du, J.; Schinazi, R. F.; Lee, D.; Newton, M. G.; Chu, C. K. *Tetrahedron Lett.* **1994**, *35*, 5405–5408.
  - (9) Nishiyama, H.; Itoh, Y.; Matsumoto, H.; Park, S.-B.; Itoh, K. *J. Am. Chem. Soc.* **1994**, *116*, 2223–2224.
  - (10) Cluet, F.; Haudrechy, A.; LeBer, P.; Sinay, P. *Synlett* **1994**, 913–915.
  - (11) Togni, A.; Venanzi, L. M. *Angew. Chem., Int. Ed. Engl.* **1994**, *33*, 497–526.
  - (12) Salaun, J.; *Curr. Med. Chem.* **1995**, *2*, 511–542.
  - (13) Doyle, M. P. In *Comprehensive Organometallic Chemistry II*, Vol. 12; Hegedus, L. S., Ed.; Pergamon: Oxford, 1995.
  - (14) Nishiyama, H.; Itoh, Y.; Sugawara, Y.; Matsumoto, H.; Aoki, K.; Itoh, K. *Bull. Chem. Soc. Jpn.* **1995**, *68*, 1247–1262.
  - (15) Park, S.-B.; Sakata, N.; Nishiyama, H. *Chem. Eur. J.* **1996**, *2*, 303–306.
  - (16) Nishiyama, H.; Aoki, K.; Itoh, H.; Iwamura, T.; Sakata, N.; Kurihara, O.; Motoyama, Y. *Chem. Lett.* **1996**, 1071–1072.
  - (17) Zampella, A.; D'Auria, M. V.; Debitus, L. M. C.; Roussakis, C. *J. Am. Chem. Soc.* **1996**, *118*, 11 085–11 088.
  - (18) Doyle, M. P.; Forbes, D. C. *Chem. Rev.* **1998**, *98*, 911–935.

- (19) Doyle, M. P.; McKervey, M. A.; Ye, T. *Modern Catalytic Methods for Organic Synthesis with Diazo Compounds*; Wiley: New York, 1998.
- (20) Doyle, M. P.; Protopopova, M. N. *Tetrahedron* **1998**, *54*, 7919–7946.
- (21) Rodriguez, A. D.; Shi, J.-G. *Org. Lett.* **1999**, *1*, 337–340.
- (22) Dale L. Boger, D. L.; Ledebner, M. W.; Kume, M.; Jin Q. *Angew. Chem. Int. Ed. Engl.* **1999**, *38*, 2424–2426.
- (23) Salaun, J. *Small Ring Compounds in Organic Synthesis*, VI; de Meijere, A., Ed.; Springer: Berlin, 2000; Vol. 207, pp 1–67.
- (24) Sanders, C. J.; Gillespie, K. M.; Scott, *Tetrahedron. Asym.* **2001**, *12*, 1055–1061.
- (25) Wipf, P.; Kendall, C.; Stephenson, C. R. J. *J. Am. Chem. Soc.* **2001**, *123*, 122–123.
- (26) Che, C. M.; Huang, J. S.; Lee, F. W.; Li, Y.; Lai, T. S.; Kwong, H. L.; Teng, P. F.; Lee, W. S.; Lo, W. C.; Peng, S. M.; Zhou, Z. Y. *J. Am. Chem. Soc.* **2001**, *123*, 4119–4129.
- (27) Fujiwara, T.; Odaira, M.; Takeda, T. *Tetrahedron Lett.* **2001**, *42*, 3369–3372.
- (28) Nagashima, T.; Davies, H. M. L. *J. Am. Chem. Soc.* **2001**, *123*, 2695–2696.
- (29) Aggarwal, V. K.; Alonso, E.; Fang, G.; Ferrara, M.; Hynd, G.; Porcelloni, M. *Angew. Chem. Int. Ed.* **2001**, *40*, 1433–1436.
- (30) Rodriguez-Garcia, C.; Oliva, A.; Ortuno, R. M.; Branchadell, V. *J. Am. Chem. Soc.* **2001**, *123*, 6157–6163.
- (31) Blomstrom, D. C.; Herbig, K.; Simmons, H. E. *J. Org. Chem.* **1965**, *30*, 959–964.
- (32) Pienta, N. J.; Kropp, P. J. *J. Am. Chem. Soc.* **1978**, *100*, 655–657.
- (33) Kropp, P. J. *Acc. Chem. Res.* **1984**, *17*, 131–137.
- (34) Wessig, P.; Muhling, O. *Angew. Chem., Int. Ed.* **2001**, *40*, 1064–1065.
- (35) Simmons, H. E.; Smith, R. D. *J. Am. Chem. Soc.* **1959**, *81*, 4256–4264.
- (36) Erdik, E. *Tetrahedron* **1987**, *43*, 2203–2212.
- (37) Takai, K.; Utimoto, K. *J. Org. Chem.* **1994**, *59*, 2671–2673.
- (38) Rubottom, G. M.; Beedle, E. C.; Kim, C.-W.; Mott, R. C. *J. Am. Chem. Soc.* **1985**, *107*, 4230–4233.
- (39) Charette, A. B.; Marcoux, J.-F. *Synlett* **1995**, 1197–1207.
- (40) Rawson, R. J.; Harrison, I. T. *J. Org. Chem.* **1970**, *35*, 2057–2058.
- (41) Friedrich, E. C.; Lewis, E. J. *J. Org. Chem.* **1990**, *55*, 2491–2494.
- (42) Furukawa, J.; Kawabata, N.; Nishimura, *Tetrahedron Lett.* **1966**, 3353–3354.
- (43) Wittig, G.; Schwarzenbach, K. *Angew. Chem.* **1959**, *71*, 652.
- (44) Denmark, S. E.; Edwards, J. P. *J. Org. Chem.* **1991**, *56*, 6974–6981.

The Simmons–Smith reaction is a popular method for synthesizing cyclopropanated products from olefins using a reagent formed from CH<sub>2</sub>I<sub>2</sub> and a Zn–Cu couple.<sup>35</sup> After the discovery of the Simmons–Smith cyclopropanation reaction,<sup>35</sup> a great deal of work has been done to improve and develop alternative methods to produce similar active reagents.<sup>36–61</sup> Many of these Simmons–Smith-type reagents and related carbenoids are thought to be formed from CH<sub>2</sub>I<sub>2</sub> (or other polyhalomethanes) and a metal atom and have general RMCH<sub>2</sub>X structures, where R is some atom or functional group, M is a metal atom like Zn, Li, or Sm, and X is a halogen atom Cl, Br, or I. A metal atom is not always required and ultraviolet photolysis of CH<sub>2</sub>I<sub>2</sub> in the presence of olefins gives cyclopropanated products with high stereospecificity and little C–H insertion reaction.<sup>31–33</sup> Several experiments observed isopolyhalomethane species following ultraviolet photolysis of polyhalomethanes in condensed phase environments.<sup>62–71</sup> Density functional theory (DFT) calculations for the reaction of isodihalomethanes (CH<sub>2</sub>X–X where X = Cl, Br, I) with ethylene<sup>72,73</sup> found they reacted with ethylene via a one step mechanism similar to that for Simmons–Smith carbenoids (XZnCH<sub>2</sub>X).<sup>51,74–82</sup> Time-resolved resonance Raman

experiments showed that CH<sub>2</sub>I–I reacts with cyclohexene solvent to form an I<sub>2</sub> leaving group on the 5–10 ns time-scale,<sup>83</sup> and this combined with theoretical results<sup>73,74</sup> indicates that CH<sub>2</sub>I–I is the carbenoid species mainly responsible for the ultraviolet photolysis of CH<sub>2</sub>I<sub>2</sub> method for cyclopropanation of olefins and a reaction mechanism was proposed.<sup>73,74,83</sup> The CH<sub>2</sub>I–I carbenoid has only one atom less than the classical Simmons–Smith type carbenoid (IZnCH<sub>2</sub>I) an interesting species to compare to Simmons–Smith type carbenoids to elucidate the role of the metal atom.<sup>80</sup>

The Simmons–Smith carbenoid (IZnCH<sub>2</sub>I) is difficult to react with highly substituted C=C bonds.<sup>33,35</sup> Many methods developed for cyclopropanation of olefins are not able to achieve total control of diastereoselectivity in the synthesis of polysubstituted cyclopropanes. Some methods require the use of toxic reagents or cannot react effectively with C=C bonds that are tri- or tetrasubstituted to make a cyclopropanated product. However, there have been experimental reports of using Sm/CH<sub>2</sub>I<sub>2</sub> reagents to make cyclopropanated allylic alcohols with complete stereospecificity with respect to the olefin geometry by Molander and co-workers<sup>54,56,57</sup> and to produce cyclopropylcarboxamides with complete stereospecificity from  $\alpha,\beta$  unsaturated amides with di-, tri- and tetrasubstituted C=C bonds by Concellón and co-workers.<sup>61</sup> Several stereoselective reactions of the Sm/CH<sub>2</sub>I<sub>2</sub> and/or the Sm/CH<sub>2</sub>Cl reagents have also been reported for cyclopropanation of allylic alcohols by Lautens and co-workers<sup>58,59</sup> and Cossy, Blanchard, Meyer.<sup>60</sup> The Sm/CH<sub>2</sub>I<sub>2</sub> carbenoid is believed to be one of the most efficient and highly diastereoselective cyclopropanating reagents.<sup>54,56,57,61</sup> Their cyclopropanation reactions are usually performed by addition of a solution of olefin and 3–4 equiv of CH<sub>2</sub>I<sub>2</sub> in THF solvent to a slurry of 3–4 equiv of Sm metal or Sm(Hg) in THF solvent at –78 °C and high yields of cyclopropanated products can be produced at low temperatures.<sup>54,56,57,61</sup> This indicates that the Sm/CH<sub>2</sub>I<sub>2</sub> carbenoid species is very reactive and much more reactive than the classical Simmons–Smith (IZnCH<sub>2</sub>I) carbenoid that requires relatively high temperatures for cyclopropanation reactions.<sup>35</sup> The high reactivity for the Sm/CH<sub>2</sub>I<sub>2</sub> cyclopropanating reagents may possibly be accounted for by assuming the formation of a Sm(II) carbenoid such as ISmCH<sub>2</sub>I. The Sm/CH<sub>2</sub>I<sub>2</sub> reagent responsible for the cyclopropanation reactions has been proposed to be the ISmCH<sub>2</sub>I species by both Molander and co-workers<sup>54,56,57</sup> and Concellón and co-workers.<sup>61</sup> Despite the synthetic importance of the Sm/CH<sub>2</sub>I<sub>2</sub> cyclopropanating reagents, there have apparently been no theoretical work reported for their reactions or for the characterization of the probable carbenoid species responsible for the reactions. It is also not clear what the role the THF solvent has in the cyclopropanation reactions. There is a compelling need for a detailed understanding of the reaction mechanism for the Sm/CH<sub>2</sub>I<sub>2</sub> promoted cyclopropanation reactions and a better knowledge of the structure and properties of the active Sm (II) carbenoid species (ISmCH<sub>2</sub>I) compared to related Simmons–Smith type carbenoids such as IZnCH<sub>2</sub>I.

- (45) Charette, A. B.; Brochu, C. *J. Am. Chem. Soc.* **1995**, *117*, 11 367–11 368.  
 (46) Yang, Z. Q.; Lorenz, J. C.; Shi, Y. *Tetrahedron Lett.* **1998**, *39*, 8621–8624.  
 (47) Charette, A. B.; Francoeur, S.; Martel, J.; Wilb, N. *Angew. Chem., Int. Ed.* **2000**, *39*, 4539–4542.  
 (48) Simmons, H. E.; Cairns, T. L.; Vladuchick, S. A.; Hoiness, C. M. *Org. React. (N. Y.)* **1973**, *20*, 1.  
 (49) Charette, A. B.; Beauchemin, A. *Org. React. (N. Y.)* **2001**, *58*, 1.  
 (50) Charette, A. B.; Gagnon, A.; Fournier, J.-F. *J. Am. Chem. Soc.* **2002**, *124*, 386–387.  
 (51) Zhao, C. Y.; Wang, D. Q.; Phillips, D. L. *J. Am. Chem. Soc.* **2002**, *124*, 12 903–12 914.  
 (52) Imamoto, T.; Takeyama, T.; Koto, H. *Tetrahedron Lett.* **1986**, *27*, 3243–3246.  
 (53) Molander, G. A.; La Belle, E.; Hahn, G. *J. Org. Chem.* **1986**, *51*, 5259–5264.  
 (54) Molander, G. A.; Etter, J. B. *J. Org. Chem.* **1987**, *52*, 3944–3946.  
 (55) Imamoto, T.; Takiyama, N. *Tetrahedron Lett.* **1987**, *28*, 1307–1308.  
 (56) Molander, G. A.; Etter, J. B.; Zinke, P. W. *J. Am. Chem. Soc.* **1987**, *109*, 453–463.  
 (57) Molander, G. A.; Harring, L. S. *J. Org. Chem.* **1989**, *54*, 3525–3532.  
 (58) (a) Lautens, M.; Delanghe, P. H. M. *J. Org. Chem.* **1992**, *57*, 798–800.  
 (b) Lautens, M.; Delanghe, P. H. M. *J. Org. Chem.* **1993**, *58*, 5037–5039.  
 (59) (a) Lautens, M.; Delanghe, P. H. M. *J. Org. Chem.* **1995**, *60*, 2474–2487.  
 (b) Lautens, M.; Delanghe, P. H. M. *J. Am. Chem. Soc.* **1994**, *116*, 8526–8535.  
 (60) Cossy, J.; Blanchard, N.; Meyer, C. *J. Org. Chem.* **1998**, *63*, 5728–5729.  
 (61) Concellón, J. M.; Rodríguez-Solla, H.; Gómez, C. *Angew. Chem., Int. Ed.* **2002**, *41*, 1917–1918.  
 (62) Maier, G.; Reisenauer, H. P. *Angew. Chem., Int. Ed. Engl.* **1986**, *25*, 819–822.  
 (63) Maier, G.; Reisenauer, H. P.; Hu, J.; Schaad, L. J.; Hess, B. A., Jr. *J. Am. Chem. Soc.* **1990**, *112*, 5117–5122.  
 (64) Tarnovsky, A. N.; Alvarez, J.-L.; Yartsev, A. P.; Sundström, V.; Åkesson, E. *Chem. Phys. Lett.* **1999**, *312*, 121–130.  
 (65) Zheng, X.; Phillips, D. L. *J. Phys. Chem. A* **2000**, *104*, 6880–6886.  
 (66) Zheng, X.; Kwok, W. M.; Phillips, D. L. *J. Phys. Chem. A* **2000**, *104*, 10 464–10 470.  
 (67) Zheng, X.; Fang, W.-H.; Phillips, D. L. *J. Chem. Phys.* **2000**, *113*, 10 934–10 946.  
 (68) Kwok, W. M.; Ma, C.; Parker, A. W.; Phillips, D.; Towrie, M.; Matousek, P.; Phillips, D. L. *J. Chem. Phys.* **2000**, *113*, 7471–7478.  
 (69) Zheng, X.; Lee, C. W.; Li, Y. L.; Fang, W.-H.; Phillips, D. L. *J. Chem. Phys.* **2001**, *114*, 8347–8356.  
 (70) Tarnovsky, A. N.; Wall, M.; Gustafson, M.; Lascoux, N.; Sundström, V.; Åkesson, E. *J. Phys. Chem. A* **2002**, *106*, 5999–6005.  
 (71) Wall, M.; Tarnovsky, A. N.; Pascher, T.; Sundström, V.; Åkesson, E. *J. Phys. Chem. A* **2003**, *107*, 211–217.  
 (72) Phillips, D. L.; Fang, W.-H.; Zheng, X. *J. Am. Chem. Soc.* **2001**, *123*, 4197–4203.  
 (73) Phillips, D. L.; Fang, W.-H. *J. Org. Chem.* **2001**, *66*, 5890–5896.  
 (74) Bernardi, F.; Bottoni, A.; and Miscione, P. *J. Am. Chem. Soc.* **1997**, *119*, 12 300–12 305.  
 (75) Dargel, T. K.; Koch, W. *J. Chem. Soc., Perkin Trans. 2* **1996**, 877–881.  
 (76) Nakamura, E.; Hirai, A.; Nakamura, M. *J. Am. Chem. Soc.* **1998**, *120*, 5844–5845.  
 (77) Harai, A.; Nakamura, M.; Nakamura, E. *Chem. Lett.* **1998**, *9*, 927–928.  
 (78) Hermann, H.; Lohrenz, J. C. W.; Kühn, A.; Boche, G. *Tetrahedron* **2000**, *56*, 4109–4115.

- (79) Boche, G.; Lohrenz, J. C. W. *Chem. Rev.* **2001**, *101*, 697–756.  
 (80) Fang, W.-H.; Phillips, D. L.; Wang, D.; Li, Y.-L. *J. Org. Chem.* **2002**, *67*, 154–160.  
 (81) Wang, D.; Phillips, D. L.; Fang, W. H. *Organometallics* **2002**, *21*, 5901–5910.  
 (82) Nakamura, M.; Hirai, A.; Nakamura, E. *J. Am. Chem. Soc.* **2003**, *125*, 2341–2350.  
 (83) Li, Y.-L.; Leung, K. H.; Phillips, D. L. *J. Phys. Chem. A* **2001**, *105*, 10 621–10 625.

We note that recent density functional theory calculations have proven very useful to elucidate the cyclopropanation reaction mechanism(s) of Simmons–Smith type carbenoids and related lithium carbenoids by a number of research groups.<sup>51,74–82</sup> To our knowledge, there have been no similar calculations done for the  $\text{ISmCH}_2\text{I}$  carbenoid species, and this is probably due to the difficulty in dealing with the lanthanide Sm atom. DFT calculations for Sm and other lanthanide complexes have only been recently reported in the literature by several different groups and are still relatively rare.<sup>84–92,104</sup> Theoretical calculations for chemical reactivity are even rarer for lanthanide complexes. To our knowledge, there have been only a few reports such as those by Maron, Eisenstein and Perrin for the H exchange and C–H activation reactions of selected lanthanide complexes<sup>89–91</sup> and by Sherer and Cramer for characterizing methane metathesis of several lanthanide complexes.<sup>92</sup>

In this paper, we present a hybrid DFT (B3LYP) study for the  $\text{ISmCH}_2\text{I} + \text{CH}_2\text{CH}_2$  cyclopropanation reactions. To our knowledge, this is the first computational study of the cyclopropanation reactions for a Sm (II) carbenoid species (or for that matter any lanthanide carbenoid species). We found the  $\text{ISmCH}_2\text{I}$  carbenoid to have a “samarium carbene” complex character with properties similar to previously investigated lithium carbenoids ( $\text{LiCH}_2\text{X}$  where  $\text{X} = \text{Cl, Br, I}$ ) but noticeably different than the closely related classical Simmons–Smith ( $\text{IZnCH}_2\text{I}$ ) carbenoid. The effect of THF solvent was also examined at the DFT level by explicit coordination of the solvent THF molecules to the Sm (II) center in the  $\text{ISmCH}_2\text{I}$  carbenoid. We briefly discuss our results in relation to other metal carbenoid reactions and experimental results for Sm/ $\text{CH}_2\text{I}_2$  promoted cyclopropanation reactions.

## Computational Details

The hybrid B3LYP or UB3LYP density functional method<sup>93–95</sup> was used to investigate the cyclopropanation reaction mechanisms of the  $\text{ISmCH}_2\text{I}$  carbenoid with ethylene. The probable effect of solvent on the reactions was explicitly considered by coordination of tetrahydrofuran (THF) molecules to the Sm (II) atom of the carbenoid species. The cyclopropanation reaction mechanism with coordination of one and two THF solvent molecules to the  $\text{ISmCH}_2\text{I}$  carbenoid are denoted as  $\text{ISmCH}_2\text{I}/(\text{THF})_n$  ( $n = 1, 2$ ) in all of the figures and tables presented here and were compared with the reactions of the parent Sm (II) carbenoid  $\text{ISmCH}_2\text{I}$  with ethylene, in which the solvent THF molecules are absent. The stationary structures of the potential energy surfaces were fully optimized with  $C_1$  symmetry at the B3LYP level of theory. Analytical frequency calculations were performed in order to confirm the optimized structures to be either a minimum or a first-order saddle-point as well as to obtain the zero-point energy correction. IRC calculations<sup>96</sup> were performed to confirm the optimized transition state correctly connects the relevant reactants and products.

Geometry optimization for all reactants, intermediates, transition states and products as well as the frequency calculations were carried out with the 6-311G\*\* basis set for the carbon and hydrogen atoms of the Sm carbenoid moiety ( $\text{CH}_2$  group) and the ethylene ( $\text{CH}_2=\text{CH}_2$ ) group. These carbon and hydrogen atoms are expected to affect the reaction barriers more than the other carbon, hydrogen, and oxygen atoms in the THF solvent molecule. Thus, a smaller 6-31G\* basis set was employed for the carbon, hydrogen and oxygen atoms of the THF solvent moiety in order to keep the calculations tractable. The lan12dz basis set<sup>97</sup> (which combines the Hay–Wadt relativistic core potential) was used for the iodide atom. The relativistic core potentials (RECPs), optimized by the Stuttgart–Dresden group,<sup>100–102</sup> were used for the Sm (II) atom. Unless specifically noted in the text, all calculations used the “large core” RECP in which 5s, 5p, and 6s electrons were explicitly treated as “valence” electrons with the remaining electrons replaced by the RECP.<sup>100,101</sup> Thus, 10 valence electrons RECP were used for the Sm (II) center. In addition, in this “large core” RECP, the partially filled 4f<sup>6</sup> electrons which do not participate actively in the bonding were also included in the core for a total of 52 electrons. The RECPs were used in combination with their optimized basis set with an additional f polarization function. The “large core” RECP basis set is denoted as 6-311A in the Results and Discussion section. The energies of the stationary structures were refined by the single-point calculations done at the B3LYP level of theory using a larger hybridized basis set referred to as 6-311B. The 6-311B basis set is composed of the standard 6-311++G\*\* basis set for C and H atoms of the Sm carbenoid moiety ( $\text{CH}_2$  group) and the ethylene ( $\text{CH}_2=\text{CH}_2$ ) group, a SDB-aug-cc-PVTZ basis set<sup>98,99</sup> that includes two sets of d, one set of f polarization functions and each set of s, p, d, f diffuse functions in conjunction with the Stuttgart–Dresden–Bonn relativistic core potential for the iodide atoms and the basis sets for the other atoms are the same as used in the 6-311A basis set. The larger hybridized basis set 6-311B is composed of 409 basis functions contracted from 755 primitive Gaussian functions for the reaction system of  $\text{ISmCH}_2\text{I}/(\text{THF})_2 + \text{C}_2\text{H}_4$ .

For comparison purposes, one set of the “small core” RECP calculations was done to compare with the corresponding “large core” RECP calculations for the  $\text{ISmCH}_2\text{I} + \text{C}_2\text{H}_4$  reaction system. The “small core” RECPs combined with their optimized basis set and one additional g polarization function for the reactants, transition states and products of the reaction system of  $\text{ISmCH}_2\text{I} + \text{C}_2\text{H}_4$  were employed on the samarium (II) atom in which the 4f<sup>6</sup> shell was explicitly treated as valence electrons.<sup>102</sup> The basis sets used remains unchanged for all the other atoms (C and H atoms for  $\text{CH}_2$  in the carbenoid moiety and  $\text{C}_2\text{H}_4$  group). All calculations were carried out using the *Gaussian 98* program suite.<sup>103</sup>

- (84) Adamo, C.; Maldivi, P. *J. Phys. Chem. A* **1998**, *102*, 6812–6820.  
 (85) Adamo, C.; Maldivi, P. *J. Phys. Chem. A* **1999**, *103*, 7554–7554.  
 (86) Maron, L.; Eisenstein, O. *J. Phys. Chem. A* **2000**, *104*, 7140–7143.  
 (87) Gordon, J. C.; Giesbrecht, G. R.; Clark, D. L.; Hay, P. J.; Keogh, D. W.; Poli, R.; Scott, B. L.; Watkin, J. G. *Organometallics* **2002**, *21*, 4726–4734.  
 (88) Clark, D. L.; Gordon, J. C.; Hay, P. J.; Martin, R. L.; Poli, R. *Organometallics* **2002**, *21*, 5000–5006.  
 (89) Eisenstein, O.; Maron, L. *J. Organomet. Chem.* **2002**, *647*, 190–197.  
 (90) Eisenstein, O.; Maron, L. *J. Am. Chem. Soc.* **2001**, *123*, 1036–1039.  
 (91) Maron, L.; Perrin, L.; Eisenstein, O. *J. Chem. Soc., Dalton Trans.* **2002**, 534–539.  
 (92) Sherer, E. C.; Cramer, C. J. *Organometallics* **2003**, *22*, 1682–1689.  
 (93) Becke, A. D. *J. Chem. Phys.* **1993**, *98*, 5648–5652.  
 (94) Becke, A. D. *Phys. Rev. A* **1988**, *38*, 3098–3100.  
 (95) Lee, C.; Yang, W.; Parr, R. G. *Phys. Rev. B* **1988**, *37*, 785–789.  
 (96) Gonzalez, C.; Schlegel, H. B. *J. Chem. Phys.* **1989**, *90*, 2154; *J. Phys. Chem.* **1990**, *94*, 5523–5527.  
 (97) (a) Dunning, T. H., Jr.; Hay, P. J. In *Modern Theoretical Chemistry*; Schafer, H. F., III., Ed.; Plenum: New York, 1976; pp 1–28. (b) Hay, P. J.; Wadt, W. R. *J. Chem. Phys.* **1985**, *82*, 270–283. (c) Wadt, W. R.; Hay, P. J. *J. Chem. Phys.* **1985**, *82*, 284–298. (d) Hay, P. J.; Wadt, W. R. *J. Chem. Phys.* **1985**, *82*, 299–310.  
 (98) Martin, J. M. L.; Sundermann, A. *J. Chem. Phys.* **2001**, *114*, 3408–3420.  
 (99) Bergner, A.; Dolg, M.; Kuechle, W.; Stoll, H.; Preuss, H. *Mol. Phys.* **1993**, *80*, 1431.  
 (100) Dolg, M.; Stoll, H.; Savin, A.; Preuss, H. *Theor. Chim. Acta* **1989**, *75*, 173–194.  
 (101) Dolg, M.; Stoll, H.; Preuss, H. *Theor. Chim. Acta* **1993**, *85*, 441–450.  
 (102) Dolg, M.; Stoll, H.; Pruss, H. *J. Chem. Phys.* **1989**, *90*, 1730–1734.  
 (103) Frisch, M. J.; Trucks, G. W.; Schlegel, H. B.; Scuseria, G. E.; Robb, M. A.; Cheeseman, J. R.; Zakrzewski, V. G.; Montgomery, J. A., Jr.; Stratmann, R. E.; Burant, J. C.; Dapprich, S.; Millam, J. M.; Daniels, A. D.; Kudin, K. N.; Strain, M. C.; Farkas, O.; Tomasi, J.; Barone, V.; Cossi, M.; Cammi, R.; Mennucci, B.; Pomelli, C.; Adamo, C.; Clifford, S.; Ochterski, J.; Petersson, G. A.; Ayala, P. Y.; Cui, Q.; Morokuma, K.; Malick, D. K.; Rabuck, A. D.; Raghavachari, K.; Foresman, J. B.; Cioslowski, J.; Ortiz, J. V.; Baboul, A. G.; Stefanov, B. B.; Liu, G.; Liashenko, A.; Piskorz, P.; Komaromi, I.; Gomperts, R.; Martin, R. L.; Fox, D. J.; Keith, T.; Al-Laham, M. A.; Peng, C. Y.; Nanayakkara, A.; Gonzalez, C.; Challacombe, M.; Gill, P. M. W.; Johnson, B.; Chen, W.; Wong, M. W.; Andres, J. L.; Gonzalez, C.; Head-Gordon, M.; Replogle, E. S.; Pople, J. A. *Gaussian 98*; Gaussian, Inc., Pittsburgh, PA, 1998.

- (104) Kaupp, M.; Schleyer, P. V. R.; Dolg, M.; Stoll, H. *J. Am. Chem. Soc.* **1992**, *114*, 8202–8208.

**Table 1.** B3LYP/6-311A and B3LYP/6-311B Calculated Relative Energies (E) with Zero-Point Energies (ZPE) Corrections Relative to the Starting Materials (SM = ISmCH<sub>2</sub>I/(THF)<sub>n</sub> + C<sub>2</sub>H<sub>4</sub>) where n = 0, 1, 2

species	B3LYP/6-311A (B3LYP/6-311B) <sup>a</sup>	B3LYP/6-311A (B3LYP/6-311B) with small core <sup>b</sup>
ISmCH <sub>2</sub> I + C <sub>2</sub> H <sub>4</sub>	0.0 (0.0)	0.0 (0.0)
RC1	-7.4 (-6.3)	-9.2 (-7.5)
TS1	5.5 (8.2)	5.1 (7.8)
TS2	9.7 (11.8)	6.1 (9.3)
IM1	-10.2 (-8.7)	
c-C <sub>3</sub> H <sub>6</sub> + SmI <sub>2</sub>	-45.9 (-44.0)	
ISmCH <sub>2</sub> I + THF + C <sub>2</sub> H <sub>4</sub>	23.3 (23.2)	
ISmCH <sub>2</sub> I/THF + C <sub>2</sub> H <sub>4</sub>	0.0 (0.0)	
RC2	-4.5 (-3.8)	
TS3	5.8 (8.2)	
TS4	10.9 (12.9)	
IM2	-8.7 (-7.6)	
c-C <sub>3</sub> H <sub>6</sub> + SmI <sub>2</sub> /THF	-48.7 (-46.5)	
ISmCH <sub>2</sub> I + 2THF + C <sub>2</sub> H <sub>4</sub>	42.6 (42.5)	
ISmCH <sub>2</sub> I/(THF) <sub>2</sub> + C <sub>2</sub> H <sub>4</sub>	0.0 (0.0)	
RC3	-2.7 (-2.3)	
TS5	6.1 (8.4)	
TS6	14.2 (15.5)	
IM3	-5.5 (-4.5)	
c-C <sub>3</sub> H <sub>6</sub> + SmI <sub>2</sub> /(THF) <sub>2</sub>	-52.2 (-48.0)	

<sup>a</sup> The values are computed from 6-311A or 6-311B (the values in parentheses) basis sets with large core RECP for Sm (see the 6-311A and 6-311B basis set descriptions in the computational details). <sup>b</sup> The values are computed from 6-311A or 6-311B (the values in parentheses) basis sets with small core RECP for Sm.

## Results

The optimized stationary structures (minima, saddle points) on the potential energy surfaces of the reactions are depicted schematically in Figures 1, 2, and 3 with selected key geometry parameters (bond lengths and bond angles). The detailed structural parameters and energies for the structures determined here are collected in the Supporting Information. The relative energies relative to the starting materials (Sm = ISmCH<sub>2</sub>I/(THF)<sub>n</sub> + C<sub>2</sub>H<sub>4</sub> where n = 0, 1, 2 with ZPE corrections with different basis sets (6-311A and 6-311B with “small core” and “large core” RECP for Sm) are tabulated in Table 1. The relative energies including ZPE for the different reaction pathways are shown graphically in Figure 4.

**A. Cyclopropanation Reaction of the Sm (II) Carbenoid ISmCH<sub>2</sub>I with Ethylene.** Figure 1 displays the optimized geometry found for the Sm (II) carbenoid ISmCH<sub>2</sub>I, the reactant complex RC1, and the transition states TS1 and TS2 for reactions with ethylene through two different pathways to produce cyclopropane (c-C<sub>3</sub>H<sub>6</sub>) and SmI<sub>2</sub>. One pathway involves a one-step methylene transfer mechanism through TS1 where the pseudotrigonal methylene group of the carbenoid adds to the ethylene π-bond to form two new C–C bonds asynchronously. This is accompanied by a 1,2-migration of the iodine anion from the carbon atom to the Sm atom. The three-centered transition state is similar to that proposed by Molander and co-workers<sup>54,56,57</sup> and Concellon and co-workers<sup>61</sup> to explain the stereochemical features of this type of reaction. Another pathway is a carbometalation process, in which a [2 + 2] addition of ethylene to the Sm–C bond for the carbenoid proceeds to produce an intermediate IM1 through a four-centered transition structure TS2. A subsequent intramolecular substitution reaction of IM1 produces the final cyclopropane product. In the methylene transfer pathway, the Sm carbenoid ISmCH<sub>2</sub>I ap-

proaches ethylene (C<sub>2</sub>H<sub>4</sub>) in an asymmetric manner and reacts with one of the CH<sub>2</sub> groups from above the molecular plane. In the carbometalation process, the ethylene molecule simultaneously moves to the Sm carbenoid to reach the Sm and C atoms in the carbenoid. A π-complex RC1 is formed when the two molecules move toward one another and can be regarded as the reactant complex for these two reaction pathways. π-type reactant complexes were also found in calculations done for lithium (LiCH<sub>2</sub>X) and Simmons–Smith type zinc (XZnCH<sub>2</sub>X) carbenoids. Recent MP2(full)/6-311++G\*\* calculations predicted a stabilization energy of 11.1 kcal/mol for the π complex of LiCH<sub>2</sub>Cl and CH<sub>2</sub>CH<sub>2</sub>.<sup>78</sup> Previous B3LYP/6-311G\*\*/B3LYP/DZVP calculations obtained a stabilization energy of 4.0 kcal/mol for the π complex of ClZnCH<sub>2</sub>Cl and CH<sub>2</sub>CH<sub>2</sub>.<sup>74</sup>

Inspection of Figure 1 shows that the geometry of the active Sm(II) carbenoid species ISmCH<sub>2</sub>I can be viewed as a complex between methylene carbene (CH<sub>2</sub>) and samarium diiodide (SmI<sub>2</sub>). The C–I<sup>1</sup> and Sm–I<sup>1</sup> bond lengths are 2.335 Å and 3.280 Å, respectively, at the large core RECP level of theory, and the corresponding bond lengths are 2.338 and 3.220 Å, respectively, at the small core RECP level of theory. Both C–I<sup>1</sup> and Sm–I<sup>1</sup> bond lengths are noticeably elongated compared to the C–I and Sm–I bond lengths in the Simmons–Smith zinc carbenoid IZnCH<sub>2</sub>I (the C–I bond length was reported to be 2.193 Å in ref 80) and SmI<sub>2</sub> (the Sm–I bond length is 3.056 Å in this work). The Sm–C–I<sup>1</sup> bond angle is only 83.4° and this is much smaller than the Zn–C–I bond angle of 111.0° in the Simmons–Smith zinc carbenoid (IZnCH<sub>2</sub>I).<sup>80</sup> The I–Sm–I bond angle of 144.5° for ISmCH<sub>2</sub>I is only slightly larger than that of the free SmI<sub>2</sub> molecule (140.2°). The H–C–Sm–H dihedral angle is calculated to be 164.7° and 164.8° at the large core and small core RECP levels of theory, respectively. This indicates the carbon atom of the Sm carbenoid is close to a sp<sup>2</sup> hybrid structure and is much different from the almost sp<sup>3</sup> hybridization structure of the carbon atom for the IZnCH<sub>2</sub>I zinc carbenoid that has a corresponding dihedral angle (H–C–Zn–H) of 124.2°. The Sm–C–H angle is 128°, and the H–C–H angle is 106.5° in the ISmCH<sub>2</sub>I carbenoid. This is consistent with the ISmCH<sub>2</sub>I carbenoid carbon atom having noticeable sp<sup>2</sup> character with the Sm–C–H angles increasing from 120° and the H–C–H angle decreasing from the about 120° expected for an sp<sup>3</sup> hybridized carbon. All of the above structural features of the Sm(II) carbenoid suggest that it has a “samarium carbene complex” structure. This is very similar to the structures obtained for several lithium carbenoid species where the H–C–Li–H dihedral angle was reported to be about 178.0° which indicates the lithium carbenoids (LiCH<sub>2</sub>X) have an almost sp<sup>2</sup> hybridization for their carbon atom.<sup>78,81</sup> The ethylene CH<sub>2</sub>CH<sub>2</sub> η<sup>2</sup> coordination to the Sm carbenoid to form the reactant complex RC1 does not significantly change the geometry of the carbenoid species except for the Sm–C and Sm–I bond lengths that become slightly elongated. The η<sup>2</sup> Sm–C bond lengths are computed to be 3.270 and 3.249 Å at the large core RECP level of theory and 3.152 and 3.170 Å at the small core RECP level of theory.

Examination of Figure 1 for the methylene transfer pathway shows the C<sup>1</sup>–C<sup>2</sup> distance in TS1 is 2.353 Å, and this is 0.234 Å shorter than the C<sup>1</sup>–C<sup>3</sup> distance (values from the large core RECP calculations). The planar ethylene molecule undergoes a significant pyramidalization of about 10.4 degrees for C<sup>2</sup> in

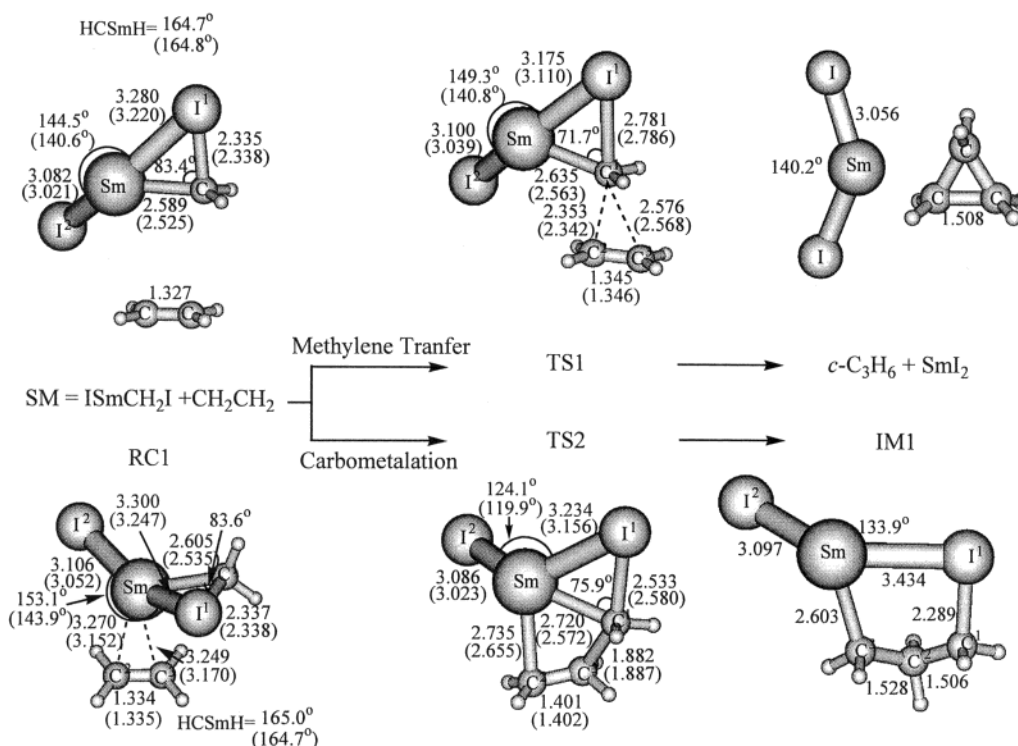


**Figure 1.** Schematic diagrams of the optimized geometry from the B3LYP/6-311A computations (see the basis sets description in the computational details) for the samarium (II) carbenoid ISmCH<sub>2</sub>I, reactant complex RC1, the intermediate IM1 as well as the transition states for the cyclopropanation with ethylene. TS1 = transition state for the methylene transfer pathway for reaction of ISmCH<sub>2</sub>I with ethylene. TS2 = transition state for carbometalation pathway for reaction of ISmCH<sub>2</sub>I with ethylene. Selected structural parameters (the geometrical parameters in parentheses are from the small core RECP calculation) are shown for each species with the bond lengths in Å and the bond angles in degrees.

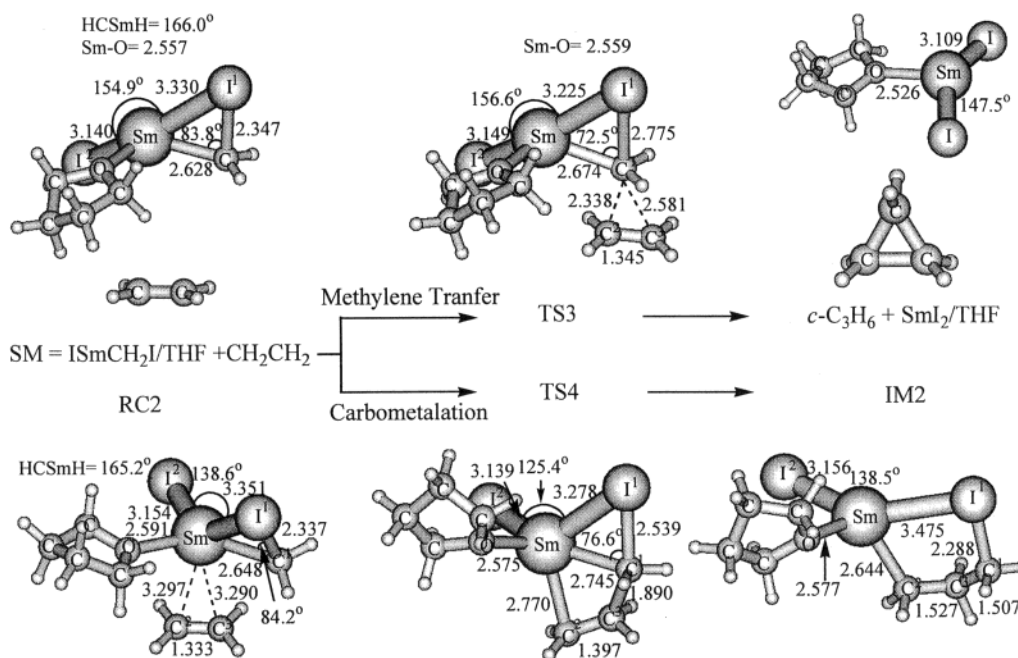


**Figure 2.** Schematic diagram of the optimized geometry from the B3LYP/6-311A computations for the one THF solvated samarium (II) carbenoids ISmCH<sub>2</sub>I/THF, the reactant complex RC2, the intermediate IM2 as well as the transition states for the cyclopropanation of ISmCH<sub>2</sub>I/THF with ethylene. TS3 = transition state for the methylene transfer pathway for the reaction of ISmCH<sub>2</sub>I/THF with ethylene. TS4 = transition state for the carbometalation pathway for reaction of ISmCH<sub>2</sub>I/THF with ethylene. Selected structural parameters are shown for each species with the bond lengths in Å and the bond angles in degrees.

the TS1 structure and this indicates the onset of the  $sp^2 \rightarrow sp^3$  rehybridization required for cyclopropane formation, whereas the pyramidalization is only 0.5 degrees for C<sup>3</sup>. This reflects the asynchronous approach of the CH<sub>2</sub>CH<sub>2</sub> molecule for the

cyclopropanation reaction. The C<sup>2</sup>=C<sup>3</sup> and C<sup>1</sup>–Sm bond lengths are elongated by 0.011 and 0.030 Å respectively upon going from the reactant complex (RC1) to the transition state (TS1). The interaction of the ISmCHI<sub>2</sub> moiety with the  $\pi$  olefin orbitals

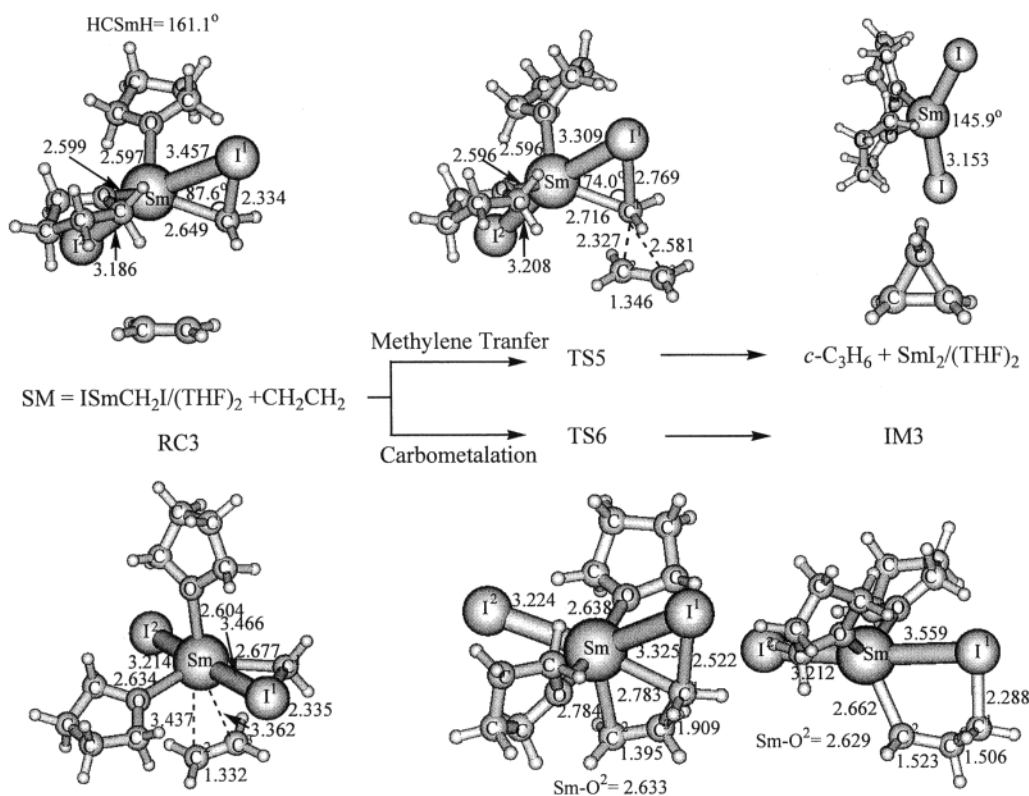


**Figure 3.** Schematic diagram of the optimized geometry from the B3LYP/6-311A computations for the two THF solvated samarium (II) carbenoids ISmCH<sub>2</sub>I/(THF)<sub>2</sub>, the reactant complex RC3, the intermediate IM3 as well as the transition states for the cyclopropanation of ISmCH<sub>2</sub>I/(THF)<sub>2</sub> with ethylene. TS5 = transition state for the methylene transfer pathway for the reaction of ISmCH<sub>2</sub>I/(THF)<sub>2</sub> with ethylene. TS6 = transition state for the carbometalation pathway for reaction of ISmCH<sub>2</sub>I/(THF)<sub>2</sub> with ethylene. Selected structural parameters are shown for each species with the bond lengths in Å and the bond angles in degrees.

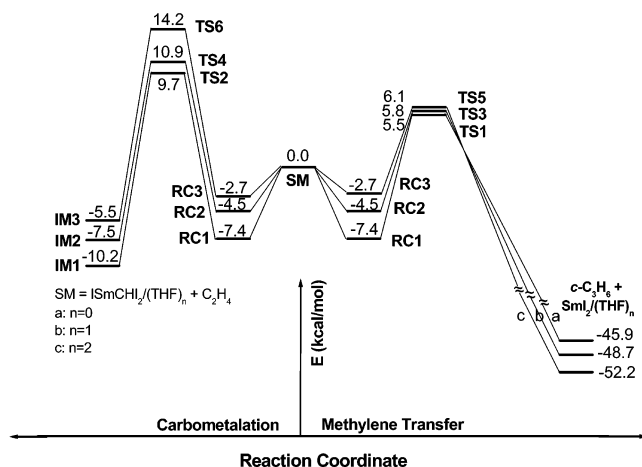


**Figure 4.** Schematic diagram showing the computed relative energies (in kcal/mol) at the B3LYP/6-311A and B3LYP/6-311B (the data in parentheses) levels for reactions of ISmCH<sub>2</sub>I/(THF)<sub>n</sub> (*n* = 0, 1, 2) with ethylene with the transition states and products energies given relative to the starting materials [SM = ISmCH<sub>2</sub>I/(THF)<sub>n</sub> + C<sub>2</sub>H<sub>4</sub> (*n* = 0, 1, 2)].

are mainly responsible for the slight lengthening of the C<sup>2</sup>=C<sup>3</sup> and C<sup>1</sup>–Sm bonds. Relatively large changes are associated with the I<sup>1</sup>–C–Sm angle, the I<sup>1</sup>–Sm–I<sup>2</sup> angle, the C<sup>1</sup>–I<sup>1</sup> and Sm–I<sup>1</sup> distances that vary from 83.4°, 153.1°, 2.337 Å, and 3.280 Å, respectively in RC1, to 71.7°, 149.3°, 2.781 Å, and 3.175 Å, respectively in TS1. Meanwhile, the C<sup>1</sup>–I<sup>1</sup> bond (2.781 Å) becomes nearly broken and the Sm–I<sup>1</sup> bond (3.175 Å) becomes almost formed in TS1. These changes in the bond lengths and bond angles are attributed to partial formation of

the SmI<sub>2</sub> byproduct in the transition state (TS1). It is evident that TS1 is the transition state of the concerted reaction from the RC1 reactant complex to c-C<sub>3</sub>H<sub>6</sub> + SmI<sub>2</sub> products. Vibrational analysis showed that the TS1 structure has one imaginary frequency (283i cm<sup>-1</sup>) and was confirmed to be the first-order saddle point connecting the corresponding reactants and products by IRC calculations.

In the carbometalation pathway, an insertion reaction of the ethylene to the Sm–C bond occurs to produce the intermediate IM1 through the four-centered TS2 transition state. The Sm–C<sup>2</sup> interaction increases significantly from 3.270 Å in RC1 to 2.735 Å in TS2. The C<sup>2</sup>–C<sup>3</sup> bond weakens somewhat from 1.334 Å in RC1 to 1.401 Å in TS2 and the C<sup>1</sup>–C<sup>3</sup> bond forms to a significant extent and goes from a distance > 3.00 Å in RC1 to 1.882 Å for TS2. This is accompanied by weakening of the C<sup>1</sup>–I and C<sup>1</sup>–Sm bonds from 2.337 Å and 2.605 Å, respectively in RC1, to 2.533 Å and 2.720 Å, respectively in TS2. The preceding changes suggest that as RC1 goes to TS2 the C–C–C moiety forms and is on its way to making a propyl group as found in IM1. The I–Sm–I angle undergoes a large change from 153.1° in RC1 to 124.1° in TS2. This suggests the Sm interaction with the C<sup>2</sup> and C<sup>3</sup> atoms increases enough to make it appear to have more four coordination character in TS2 than in TS1, which still has a large I–Sm–I angle of 149.3°. These changes in structure as RC1 goes to TS2 appear somewhat larger than that experienced as RC1 goes to TS1, which was discussed in the preceding paragraph. This suggests there may be a larger barrier for RC1 to TS2 than to TS1. Vibrational analysis found that the optimized TS2 structure had

one imaginary frequency ( $364.4i\text{ cm}^{-1}$ ) and TS2 was confirmed to be the first-order saddle-point connecting the corresponding reactants and products by IRC calculations.

Inspection of Table 1 and Figure 4 shows the reaction for the methylene transfer pathway has a barrier of 5.5 kcal/mol (with ZPE correction) and is exothermic by about 45.9 kcal/mol at the B3LYP/6-311A level. These values are relative to the separated reactants of  $\text{ISmCH}_2\text{I}$  and  $\text{CH}_2\text{CH}_2$ . The barrier becomes 5.1 kcal/mol with ZPE corrections at the B3LYP/6-311A level with a small core RECP basis set for the Sm atom. The B3LYP single point calculations using the 6-311B basis set gave results in reasonable agreement with those found for the 6-311A basis set. The relative energies at the B3LYP/6-311B systematically increase by 0.4 to 4.2 kcal/mol for all the stationary structures compared to the B3LYP/6-311A relative energies. However, the systematic increase in energy in the B3LYP/6-311B calculations does not change the relative order of the actual reaction barrier heights for the methylene transfer and carbometalation pathways. For example, the reaction barrier heights at the B3LYP/6-311B level for the reaction system of  $\text{ISmCH}_2\text{I} + \text{C}_2\text{H}_4$ ,  $\text{ISmCH}_2\text{I}/\text{THF} + \text{C}_2\text{H}_4$  and  $\text{ISmCH}_2\text{I}/(\text{THF})_2 + \text{C}_2\text{H}_4$  are calculated to be 14.5, 12.0, and 10.7 kcal/mol, respectively for the methylene transfer pathway. This is only an increase of 1.0 to 1.9 kcal/mol compared to the calculated reaction barrier heights (13.5, 10.3, 8.8 kcal/mol) for the B3LYP/6-311A computations. For the carbometalation pathway, the reaction barrier heights at the B3LYP/6-311B level for the reaction system of  $\text{ISmCH}_2\text{I} + \text{C}_2\text{H}_4$ ,  $\text{ISmCH}_2\text{I}/\text{THF} + \text{C}_2\text{H}_4$ , and  $\text{ISmCH}_2\text{I}/(\text{THF})_2 + \text{C}_2\text{H}_4$  are calculated to be 18.1, 16.1, and 17.8 kcal/mol, respectively, similar to the corresponding values (17.1, 15.4, 16.9 kcal/mol) of the B3LYP/6-311A calculations. This suggests that the B3LYP/6-311A calculations using a large core RECP for the Sm atom are reasonably reliable for further calculations of larger systems to predict reaction barriers for the methylene and carbometalation pathways. The reaction barriers of B3LYP/6-311A and B3LYP/6-311B calculations for the methylene transfer pathway are also in good agreement with the calculated value (the data shown in the last column of Table 1) from the corresponding calculations that make use of a small core RECP basis set for the Sm atom. This suggests the reaction barriers obtained using the large core RECP basis set for the Sm atom are reliable and the 4f electrons likely do not participate actively in the bonding and do not contribute substantially in these reactions. Inspection of Table 1 and Figure 4 suggests that both the methylene transfer and carbometalation mechanisms are competing pathways for the Sm (II) promoted cyclopropanation reactions. The relative order of the reaction barriers for the two reaction pathways are predicted to be the same for the different basis sets (either large core or small core RECP for the Sm atom and the 6-311A basis set compared to the 6-311B basis set). The B3LYP/6-311A calculation results will be mainly used hereafter.

The relatively low barriers found for the two different pathways for the Sm promoted ( $\text{ISmCH}_2\text{I}$ ) cyclopropanation reactions can mainly be attributed to the following two reasons. First, there are only relatively small structural changes for the Sm (II) carbenoid ( $\text{ISmCH}_2\text{I}$ ) moiety upon going from the reactant complex to the transition states. Thus, not much energy is needed to go from the reactant complex to the transition states. Second, the Sm (II) carbenoid ( $\text{ISmCH}_2\text{I}$ ) has strong electro-

philic character. NBO analysis obtained from the large core RECP calculations indicates that the natural charges on Sm atom are 1.701 for  $\text{ISmCH}_2\text{I}$  and 1.698 for RC1. This is similar to the lithium carbenoids  $\text{LiCH}_2\text{X}$  ( $\text{X} = \text{F}, \text{Cl}, \text{Br}, \text{I}$ ) and lanthanide (II) metallocenes including  $\text{Sm(II)Cp}_2$ .<sup>104</sup> The NBO charge for Sm(II) of about 1.7 for  $\text{ISmCH}_2\text{I}$  is similar to the charge for Sm(II) of about 1.899 for the  $\text{SmCp}_2$  complex.<sup>104</sup>

The existence of a stable precursor complex between the carbenoid and ethylene would increase the reaction barriers. As seen in Figure 1 and Table 1, the reactant complex RC1 is lower in energy by 7.4 kcal/mol at the B3LYP/6-311A level of theory than the starting materials (SM). This stabilization energy becomes 9.2 kcal/mol for the analogous calculations that use the small core RECP basis set for the Sm atom. These calculations indicate that the actual reaction barriers would be increased by 7–10 kcal/mol from the reactant complex compared to the barriers calculated from the SM. However, this is probably not the actual case in solutions. We know that the cyclopropanation reactions usually occur in polar solvents, for instance, the THF solvent is used for most of the Sm (II)/ $\text{CH}_2\text{I}_2$  promoted cyclopropanation reactions. These solvent molecules would be expected to have stronger coordination ability to the metal center compared to the ethylene molecule (or other olefin molecule). This will likely block the coordination of ethylene (or olefin) to the metal center or at least decrease the stabilization energy between the carbenoid and ethylene. We shall discuss the THF solvent effect in more detail in the next section.

**B. Cyclopropanation Reactions of THF Solvated Sm (II) Carbenoids  $\text{ISmCH}_2\text{I}/(\text{THF})_n$  ( $n = 1, 2$ ) with Ethylene: Why is THF Used as a Solvent for Sm(II) Carbenoid Promoted Cyclopropanation Reactions?** Cyclopropanation reactions are usually done in polar organic solvents for a number of carbenoid reagents. For the Sm promoted cyclopropanation reactions, THF is almost exclusively used as the solvent. THF has also been found to be a ligand in most reported Sm(II) crystal structures.<sup>105–107</sup> Here, we present a detailed computational investigation of the Sm(II) promoted cyclopropanation reactions by explicitly coordinating one and two THF molecules to the Sm (II) atom. Figure 2 depicts the optimized geometries found for the one THF solvated starting materials (SM =  $\text{ISmCH}_2\text{I}/\text{THF} + \text{CH}_2\text{CH}_2$ ), the  $\pi$ -type reactant complex RC2, the intermediate IM2, and the corresponding transition states TS3 and TS4. Inspection of Figure 2 shows that the formation of the solvated carbenoid species  $\text{ISmCH}_2\text{I}/\text{THF}$  with one THF solvent molecule coordinated to the Sm atom does not significantly change the geometry of most of the carbenoid moiety  $\text{ISmCH}_2\text{I}$  except for the Sm–C, Sm–I<sup>1</sup> and Sm–I<sup>2</sup> bond lengths that become slightly elongated by 0.04–0.06 Å. The H–C–Sm–H dihedral angle in the  $\text{ISmCH}_2\text{I}/\text{THF}$  complex is calculated to be  $166.0^\circ$ , and this is  $1.3^\circ$  larger than that of the  $\text{ISmCH}_2\text{I}$  complex, indicating a slight change of hybridization for the carbon atom. A  $\pi$ -type reactant complex RC2 can also be formed when an ethylene molecule coordinates to the Sm (II) center of the one THF solvated carbenoid species  $\text{ISmCH}_2\text{I}/\text{THF}$ . The formation of the  $\pi$  complex RC2 causes a significant decrease of the

(105) Evans, W. J.; Grate, J. W.; Choi, H. W.; Bloom, I.; Hunter, W. E.; Atwood, J. L. *J. Am. Chem. Soc.* **1985**, *107*, 941–946.

(106) Evans, W. J.; Drummond, D. K.; Zhang, H. M.; Atwood, J. L. *Inorg. Chem.* **1988**, *27*, 575–579.

(107) Giesbrecht, G. R.; Cui, C. M.; Shafir, A.; Shafir, A.; Arnold, J. *Organometallics* **2002**, *21*, 3841–3844.



I<sup>1</sup>–Sm–I<sup>2</sup> angle, which becomes 138.6° from 154.9° in ISmCH<sub>2</sub>I/THF complex. The interaction of the ISmCH<sub>2</sub>I moiety with the  $\pi$  olefin orbitals is also responsible for a slight lengthening of the Sm–C, Sm–I<sup>1</sup>, SmI<sup>2</sup>, Sm–O and C<sup>2</sup>–C<sup>3</sup> bonds in RC2, which are shortened by 0.01–0.03 Å compared to the ISmCH<sub>2</sub>I/THF species. The H–C–Sm–H dihedral angle in RC2 is predicted to be 165.2°, and this is only 0.5° larger than that of the ISmCH<sub>2</sub>I/THF species.

Similar to the reaction of the parent Sm(II) carbenoid ISmCH<sub>2</sub>I with ethylene, the one THF solvated reaction of ISmCH<sub>2</sub>I/THF + CH<sub>2</sub>CH<sub>2</sub> occurs through two competing pathways: methylene transfer and carbometalation. Vibrational analysis showed that the optimized TS3 and TS4 structures each have one imaginary frequency of 286i cm<sup>-1</sup> and 362.6i cm<sup>-1</sup> respectively. These transition state structures were confirmed to be the first-order saddle point connecting the corresponding reactants and products by IRC calculations. The structural changes taking place during the methylene transfer and carbometalation for the ISmCH<sub>2</sub>I/THF + CH<sub>2</sub>CH<sub>2</sub> system are similar to those found for the reactions without THF present. There are some modest differences in the structural changes for the ISmCH<sub>2</sub>I/THF + CH<sub>2</sub>CH<sub>2</sub> system that can be attributed to the coordination of THF to the Sm atom.

Examination of Table 1 and Figure 4 shows the one THF solvated reaction for the methylene transfer pathway has a barrier of 5.8 kcal/mol (with ZPE correction) and is exothermic by about 48.7 kcal/mol relative to the starting materials. The barrier increases by only 0.3 kcal/mol due to explicit coordination of one THF solvent molecule to the parent samarium carbenoid. On the other hand, the reaction for the carbometalation pathway has a higher barrier of 10.9 kcal/mol including the ZPE correction for the B3LYP/6-311A calculations. The barrier increases by 1.2 kcal/mol compared to the corresponding unsolvated reaction. In addition, coordination of one THF solvent molecule stabilizes the Sm carbenoid by 23.3 kcal/mol compared to the unsolvated Sm carbenoid. The stabilization energy (4.5 kcal/mol) coming from the interaction between the one THF solvated carbenoid and ethylene was decreased significantly by 2.9 kcal/mol. Therefore, the actual barrier for the methylene transfer pathway becomes 10.3 kcal/mol and this is decreased by 3.2 kcal/mol compared to the analogous barrier for the unsolvated case (13.5 kcal/mol). This enhanced reactivity should be the composite effect of the stabilization of the solvated Sm carbenoid species and the destabilization of the solvated Sm carbenoid species with ethylene reactant complex which comes from the incorporation of the THF solvent molecule. The strong interaction (23.3 kcal/mol for one THF solvent) between the oxygen atom in THF and the Sm(II) atom weakens the interaction of the Sm carbenoid species with ethylene. The increased reactivity for the reaction can also be readily understood by an increase in the electrophilic character of the solvated Sm carbenoid species. NBO analysis reveals that the natural charges for the Sm atom are increased from 1.701 and 1.698 in ISmCHI<sub>2</sub> and RC1 to 1.724 and 1.719 in ISmCH<sub>2</sub>I/THF and RC2, respectively. The group charges for SmCH<sub>2</sub>I<sup>1</sup>, which is supposed to be responsible for the reactivity of the carbenoid species, are also increased from 0.818 and 0.812 in ISmCHI<sub>2</sub> and RC1 to 0.825 and 0.818 in ISmCHI<sub>2</sub>/THF and RC2, respectively. The charge increase of the Sm atom in the solvated carbenoids could be accounted for by greater ionic

character for the Sm atom compared to the unsolvated carbenoids as more THF solvent molecules are coordinated to the Sm(II) carbenoids. As THF molecules are coordinated to the carbenoids, both the Sm–I and Sm–C bonds are weakened as shown in Figures 2 and 3 and the negative charges in both the I<sup>1</sup> and I<sup>2</sup> atoms become more negative, indicating a more carbene-like complex for the THF-solvated carbenoids. Schleyer and co-workers<sup>104</sup> also suggested the Sm(II) atom for the SmCp<sub>2</sub> complex has noticeable ionic character.

Figure 3 displays the optimized geometry found for the two THF solvated Sm (II) carbenoid ISmCH<sub>2</sub>I/(THF)<sub>2</sub>, the reactant complex RC3 and the transition states TS5 and TS6 for the reactions with ethylene through two different pathways to produce *c*-C<sub>3</sub>H<sub>6</sub> and SmI<sub>2</sub>/(THF)<sub>2</sub>. As shown in Table 1 and Figure 4, the two THF solvated reaction of ISmCH<sub>2</sub>I/(THF)<sub>2</sub> + CH<sub>2</sub>CH<sub>2</sub> has a barrier of 6.1 kcal/mol and is exothermic by about 52.2 kcal/mol for the methylene transfer pathway. The barrier increases by another 0.3 kcal/mol due to explicit coordination of the second THF solvent molecule to the one THF solvated Sm carbenoid. The reaction for the carbometalation pathway has a higher barrier of 14.2 kcal/mol. The barrier increases significantly by 3.3 kcal/mol compared to the corresponding one THF solvated reaction. Similar to one THF solvated reaction, the coordination of a second THF solvent molecule stabilizes the samarium carbenoid by 42.6 kcal/mol compared to the unsolvated Sm carbenoid and this is only slightly smaller than the twice (<2 × 23.2 kcal/mol) stabilization energy of the one THF solvated carbenoid species. The stabilization energy of 2.7 kcal/mol between the two THF solvated carbenoid and ethylene was further decreased by another 1.5 kcal/mol compared to the one THF solvated carbenoid system. The actual barrier for the methylene transfer pathway becomes 8.8 kcal/mol and this is decreased by another 1.5 kcal/mol compared to the actual barrier for the one THF solvated carbenoid species (10.3 kcal/mol). It is expected that coordination of a third THF solvent molecule would stabilize the carbenoid species further and decrease the stabilization energy of the  $\pi$  reactant complex further. Upon saturation of the Sm (II) center by coordination of THF solvent molecules one by one, the reactivity of the solvated carbenoid species would become relatively constant. We note the actual barriers of the unsolvated and solvated reactions for the methylene transfer pathway can be reasonably described as an exponential decay process as the number of THF goes from  $n = 0$  to  $n = 2$  as shown in Figure 5. However, the actual reaction barriers for the carbometalation pathway do not appear to change substantially or with a clear trend by coordination of THF solvent molecules. To examine bulk solvation effects, the polarized continuum (PCM) solvation model<sup>111</sup> was utilized for THF ( $\epsilon = 7.58$ ) to the unsolvated reaction system (RC1, TS1, and TS2) at the B3LYP/6-311B level. The reaction barriers from RC1 to TS1 and TS2 were computed to be 9.0 and 12.7 kcal/mol with ZPE corrections for the methylene transfer and carbometalation pathways, respectively. These results are

(108) Arduengo, A. J., III.; Tamm, M.; McLain, S. J.; Calabrese, J. C.; Davidson, F.; Marshall, W. J. *J. Am. Chem. Soc.* **1994**, *116*, 7927–7928.

(109) Kasani, A.; Michael, F.; Ronald, G. C. *J. Am. Chem. Soc.* **2000**, *122*, 726–727.

(110) Evans, W. J.; Perotti, J. M.; Brady, J. C.; Ziller, J. W. *J. Am. Chem. Soc.* **2003**, *125*, 5204–5212.

(111) (a) Miertus, S.; Scrocco, E.; Tomasi, J. *Chem. Phys.* **1981**, *55*, 117. (b) Miertus, S.; Tomasi, J. *Chem. Phys.* **1982**, *65*, 239. (c) Cossi, M.; Barone, V.; Cammi, R.; Tomasi, J. *Chem. Phys. Lett.* **1996**, *255*, 327.

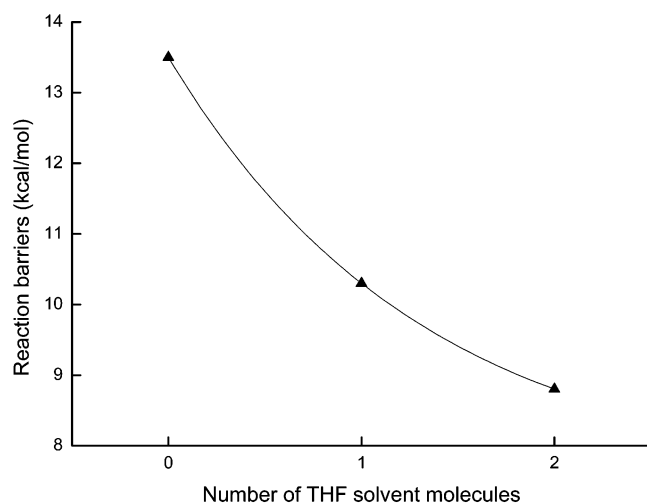


**Figure 5.** Barriers (B3LYP/6-311B, kcal/mol) to reaction calculated from the reactant complex to the transition state for the reactions of  $\text{ISmCH}_2\text{I}/(\text{THF})_n$  ( $n = 0, 1, 2$ ) with ethylene for the methylene transfer pathway as a function of the number of THF molecules.

consistent with the calculated actual reaction barriers of 10.7 and 17.8 kcal/mol from RC3 to TS5 and TS6 at the B3LYP/6-311B level, in which two THF molecules were coordinated to the Sm atom of reaction systems. This is also consistent with the barrier trend demonstrated in Figure 5 for the exponential decay of the methylene transfer pathway as a function of the number of THF molecules and can be regarded as a best limit as two more THF molecules are coordinated to the Sm(II) carbenoid.

There are some systematic changes in the structure, the charge distribution and the relative energies for the Sm carbenoid species, the reactant complexes, the intermediates, the transition states and the final products as a function of THF solvent molecules added to the system. For instance, the bond distances of  $\text{Sm}-\text{C}^1$ ,  $\text{Sm}-\text{I}^1$ ,  $\text{Sm}-\text{I}^2$ ,  $\text{Sm}-\text{C}^2$  and  $\text{Sm}-\text{C}^3$  in the carbenoids  $\text{ISmCH}_2\text{I}/(\text{THF})_n$  ( $n = 0, 1, 2$ ), RC1, RC2, RC3, methylene transfer transition states TS1, TS3, and TS5 and carbometalation transition states TS2, TS4, and TS6 (including the  $\text{C}^1-\text{C}^3$  distances for the carbometalation pathway) become systemically elongated as the number of THF goes from  $n = 0$  to 2 with no exception. The bond angles  $\text{I}^1-\text{Sm}-\text{I}^2$  and  $\text{I}^1-\text{C}^1-\text{Sm}$  become systemically larger for the above-mentioned structures as the number of THF molecules goes from  $n = 0$  to 2 with an exception that the bond angle  $\text{I}^1-\text{Sm}-\text{I}^2$  in RC1 is smaller than in RC2. However, the bond distances of  $\text{C}^1-\text{I}^1$  and  $\text{C}^1-\text{C}^2$  become systemically shortened in the methylene transfer transition states TS1, TS3, and TS5. The  $\text{C}^1-\text{I}^1$  distances in the carbenoid species and reactant complexes with ethylene remain almost the same. The Sm related bond distances for the intermediates IM1, IM2, and IM3 and by-products  $\text{SmI}_2(\text{THF})_n$  ( $n = 0, 1, 2$ ) exhibit similar trends as the number of THF goes from  $n = 0$  to 2. The natural charge distribution for the Sm atom and the group  $\text{SmC}^1\text{H}_2\text{I}^1$  becomes more positive as the number of THF goes from  $n = 0$  to 2. Energetically, the actual reaction barriers become smaller and the reaction enthalpies become more exothermic for the methylene transfer pathway as the number of THF goes from  $n = 0$  to 2, indicating the methylene transfer is the favored pathway. However, for the carbometalation pathway, the actual reaction barriers have no specific trend and the reaction enthalpies for

formation of IM1, IM2, and IM3 become less and less exothermic, suggesting it is not the favored pathway for the reactions.

## Discussion

We note that our predicted Sm (II) carbenoid species can be described as tetracoordinated or pentacoordinated Sm (II) complexes. The  $\pi$  complex RC2 can be best described as a distorted tetrahedron with four different ligands,  $\text{CH}_2\text{I}^1$ , ethylene group,  $\text{I}^2$  and one THF. The  $\pi$  complex RC3 can be described as a distorted trigonal bipyramid, with one THF and ethylene occupying the axial positions, and  $\text{I}^2$ , one THF and  $\text{CH}_2\text{I}^1$  group occupying in equatorial positions. We compare selected geometry parameters for the Sm carbenoids to those found experimentally for other Sm(II) complexes in the Supporting Information.<sup>105–110</sup>

Our studies indicate that the reactions promoted by the Sm (II) carbenoid ( $\text{ISmCH}_2\text{I}$ ) occur with relatively low barriers to the methylene transfer pathway which is moderately more favored than the carbometalation pathway. The reaction barriers computed for the methylene transfer pathway (12.9 to 8.8 kcal/mol depending on how many THF molecules are coordinated to the Sm atom) are in reasonable agreement with experimental reaction conditions that show the cyclopropanation reaction can take place at low temperatures such as  $-78^\circ\text{C}$ .<sup>54,56,57,61</sup> It is worth noting that the reactivity for the Sm (II) carbenoid ( $\text{ISmCH}_2\text{I}$ ) is similar to that found previously for several lithium carbenoids ( $\text{LiCH}_2\text{X}$  where  $\text{X} = \text{Cl}, \text{Br}, \text{I}$ ).<sup>77,78,81</sup> Recent MP2-(full)/6-311++G\*\* calculations predicted a barrier of 6.9 kcal/mol for the reaction of  $\text{LiCH}_2\text{Cl} + \text{CH}_2\text{CH}_2$ .<sup>78</sup> We note that the lithium carbenoid reactions experimentally take place at low temperatures (e.g.,  $-78^\circ\text{C}$ )<sup>104–106</sup> and these reaction conditions are very similar to those used for some of the Sm (II) carbenoid ( $\text{ISmCH}_2\text{I}$ ) cyclopropanation reactions.<sup>54,56,57,61</sup> The similar reaction barriers and reaction conditions for the lithium and Sm (II) carbenoids implies there are some similarities in the chemical reactivity for these two kinds of carbenoids and this is reasonably consistent with our present computational results. From the viewpoint of the  $\text{H}-\text{C}-\text{M}-\text{H}$  dihedral angle ( $\text{M} = \text{Li}, \text{Sm}, \text{Zn}$  and values of  $178^\circ$ ,  $164.7^\circ$ , and  $124.2^\circ$ , respectively), the carbon atom in the  $\text{ISmCH}_2\text{I}$  and  $\text{LiCH}_2\text{X}$  carbenoid species has more  $sp^2$  character than that in the Simmons–Smith  $\text{IZnCH}_2\text{I}$  carbenoid. This feature as well as the detailed structural information discussed in section A indicate the  $\text{ISmCH}_2\text{I}$  carbenoid can be considered to be a “samarium carbene complex” with properties similar to the lithium carbenoids. Our calculations for the  $\text{ISmCH}_2\text{I}$  carbenoid also indicate it undergoes only relatively small structural changes from the reactant complexes to the methylene transfer transition states implying that not much energy is required to go from the reactant complexes to their transition state. We also found the  $\text{ISmCH}_2\text{I}$  carbenoid has stronger electrophilic character than the Simmons–Smith carbenoid ( $\text{IZnCH}_2\text{I}$ ). These results help provide a reasonable explanation for why the  $\text{ISmCH}_2\text{I}$  carbenoid is experimentally substantially more reactive than the classic Simmons–Smith ( $\text{IZnCH}_2\text{I}$ ) carbenoid.

Sm (II) carbenoid ( $\text{ISmCH}_2\text{I}$ ) cyclopropanation reactions are mainly done in THF solvent experimentally.<sup>54,56,57,61</sup> We explored the role of THF solvent on the  $\text{ISmCH}_2\text{I}$  cyclopropanation reactions by explicitly coordinating one and two THF

molecules to the Sm atom. These calculations exhibited an interesting trend for the methylene reaction pathway as the THF solvent molecules were added to the system. The ISmCH<sub>2</sub>I/(THF)<sub>n</sub> (where *n* = 0,1,2) carbenoid reactant complexes with ethylene (RC1–RC3) were found to be less stable (going from –7.4 kcal/mol for RC1 to –2.7 kcal/mol for RC3) relative to their starting material (SM = ISmCH<sub>2</sub>I/THF + CH<sub>2</sub>=CH<sub>2</sub>), whereas the transition states (TS1, TS3, and TS5) changed only modestly from about 5.5 kcal/mol for TS1 to 6.1 kcal/mol for TS5. This leads the barriers for the cyclopropanation reactions to become systematically lower as more THF solvent is added (from 12.9 kcal/mol for no THF molecules to 10.3 kcal/mol for one THF molecule and 8.8 kcal/mol for two THF molecules). In contrast, the transition states for the carbometalation pathway tend to become noticeably higher and range from 9.7 kcal/mol for no THF molecules to 10.9 kcal/mol for one THF molecule and 14.2 kcal/mol for two THF molecules. This leads the reaction barriers for cyclopropanation via the carbometalation pathway to remain high (17.1 kcal/mol for zero THF, 15.4 kcal/mol for one THF and 16.9 kcal/mol for two THF molecules). These results suggest the THF solvent helps make the methylene pathway substantially more favorable than the carbometalation pathway.

The incorporation of the THF solvent molecules into the ISmCH<sub>2</sub>I/(THF)<sub>n</sub> (where *n* = 0,1,2) carbenoid results in moderate destabilization of the solvated Sm carbenoid with ethylene reactant complex species (RC2 and RC3) relative to the starting materials. This is likely due to the strong interaction of the oxygen atom in THF with the Sm(II) atom that then weakens the interaction of the Sm carbenoid species with ethylene. The increased reactivity for the ISmCH<sub>2</sub>I/(THF)<sub>n</sub> (*n* = 1,2) carbenoid reactions can also be partially attributed to there being an increase of the electrophilic character of the solvated Sm carbenoid species where the natural charges for the Sm atom and the group charges for the SmCH<sub>2</sub>I<sup>1</sup> moiety are systematically increased from ISmCHI<sub>2</sub>, ISmCHI<sub>2</sub>/THF to ISmCHI<sub>2</sub>/(THF)<sub>2</sub> and/or from RC1, RC2, to RC3 as found from NBO analysis. This suggests that as THF is added to the ISmCH<sub>2</sub>I/(THF)<sub>n</sub> (*n* = 0,1,2) carbenoid the olefin molecule reactant complex becomes less stable and can be displaced by the THF solvent in a fully solvated carbenoid species found in THF solvent. There is recent experimental evidence to support this view for the role of the THF solvent in the Sm (II) carbenoid cyclopropanation reactions. Evans and co-workers<sup>110</sup> synthesized several unsolvated lanthanide metallocenes containing tethered olefin cyclopentadienyl ligand, [(C<sub>5</sub>Me<sub>4</sub>)SiMe<sub>2</sub>(CH<sub>2</sub>CH=CH<sub>2</sub>)<sub>2</sub>]-Ln (where Ln = Sm, Eu, Yb), with the olefin oriented toward the metal in the solid state. As THF solvent was added to the [(C<sub>5</sub>Me<sub>4</sub>)SiMe<sub>2</sub>(CH<sub>2</sub>CH=CH<sub>2</sub>)<sub>2</sub>Sm complex the alkene NMR proton and carbon resonances were shifted significantly consistent with THF solvent displacing the olefin in the solution phase. This is not unexpected since THF would be expected to be a better donor than the olefin and could displace it. The interaction between the solvated carbenoid and ethylene becomes weaker as THF molecules are added. This makes the reactant

complex have character becoming more similar to that of the corresponding separated solvated carbenoid and ethylene molecule. The strong interaction between the Sm atom and THF molecules combined with coordination of the THF molecules to the Sm atom appears to block the carbometalation pathway. This is consistent with the changes we observe in the ISmCH<sub>2</sub>I/(THF)<sub>n</sub> (*n* = 0,1,2) carbenoid with olefin molecule reactant complexes as THF molecules are added to the system in our present computational study and the recent experimental results of Evans and co-workers<sup>110</sup> for the behavior of the [(C<sub>5</sub>Me<sub>4</sub>)-SiMe<sub>2</sub>(CH<sub>2</sub>CH=CH<sub>2</sub>)<sub>2</sub>Sm complex as THF solvent is added.

## Conclusion

A theoretical investigation of the cyclopropanation reactions of the ISmCH<sub>2</sub>I carbenoid with ethylene was given. The ISmCH<sub>2</sub>I carbenoid was found to possess a “samarium carbene complex” character with a structure, properties, and chemical reactivity similar to previously studied lithium carbenoids (LiCH<sub>2</sub>X where X = Cl, Br, I) but significantly different from the related classical Simmons–Smith carbenoid (IZnCH<sub>2</sub>I). This helps explain why the ISmCH<sub>2</sub>I carbenoid cyclopropanation reactions are able to occur at low temperatures. The ISmCH<sub>2</sub>I carbenoid cyclopropanation reactions could proceed via a methylene transfer pathway or a carbometalation pathway. The effect of THF solvent on the cyclopropanation reactions was investigated by additional calculations using explicit coordination of the solvent THF molecules to the Sm (II) center in the ISmCH<sub>2</sub>I carbenoid. The barriers for the ISmCH<sub>2</sub>I/(THF)<sub>n</sub> (where *n* = 0,1,2) carbenoid methylene transfer pathway reactions became progressively lower as additional THF molecules were added with the barrier decreasing from 12.9 kcal/mol for ISmCH<sub>2</sub>I to 8.8 kcal/mol for ISmCH<sub>2</sub>I/(THF)<sub>2</sub>. However, the barriers to reaction for the carbometalation pathway stayed relatively high (> 15 kcal/mol). These results suggest that the THF solvent helps to enhance the chemical reactivity of the ISmCH<sub>2</sub>I/(THF)<sub>n</sub> carbenoids toward olefins. The strong interaction between the oxygen atom in the THF molecule and the Sm(II) atom weakens the interaction of the Sm carbenoid species with ethylene. This destabilizes the reactant complexes while inducing an increase of the electrophilic character of the solvated Sm carbenoid species and these two effects appear mainly responsible for the increased reactivity for the carbenoid reactions in THF solvent.

**Acknowledgment.** This research has been supported by grants from the Research Grants Council of Hong Kong (HKU/7087/01P) to D.L.P.

**Supporting Information Available:** Selected output from the DFT calculations showing the Cartesian coordinates, total energies and vibrational zero-point energies for the ISmCH<sub>2</sub>I/(THF)<sub>n</sub> (*n* = 0,1,2) carbenoid reactants, transition states and products for the cyclopropanation reactions investigated here and shown in Figures 1–4. This material is available free of charge via the Internet at <http://pubs.acs.org>.

JA030280T